



ORIGINAL ARTICLE OPEN ACCESS

Intra Oral Photogrammetry: Trueness Evaluation of Novel Technology for Implant Complete-Arch Digital Impression In Vitro

Alessandro Pozzi^{1,2,3,4}  | Andrea Laureti^{5,6} | Isaac Tawil⁷ | James Chow⁸ | Luis Azevedo^{6,9}  | Vincent Fehmer⁶ | Irena Sailer⁶

¹Department of Clinical Science and Translational Medicine, University of Rome Tor Vergata, Rome, Italy | ²Goldstein Center for Esthetic and Implant Dentistry, Department of Restorative Sciences, The Dental College of Georgia at Augusta University, Augusta, Georgia, USA | ³Department of Periodontics and Oral Medicine, University of Michigan School of Dentistry, Ann Harbor, Michigan, USA | ⁴Department of Restorative Dentistry and Biomaterials Sciences, Harvard School of Dental Medicine, Boston, Massachusetts, USA | ⁵Department of Chemical Science and Technologies, University of Rome Tor Vergata, Rome, Italy | ⁶Division of Fixed Prosthodontics and Biomaterials, University Clinics for Dental Medicine, University of Geneva, Geneva, Switzerland | ⁷Private Practice, New York, New York, USA | ⁸Brånemark Osseointegration Centre, Hong Kong SAR-China, Hong Kong, People's Republic of China | ⁹Center for Interdisciplinary Research in Health, The Catholic University of Portugal (UCP), Viseu, Portugal

Correspondence: Alessandro Pozzi (profpozzi@me.com)

Received: 22 February 2025 | **Revised:** 15 March 2025 | **Accepted:** 27 April 2025

Keywords: dental implant | digital impression | intraoral photogrammetry | IOS | photogrammetrycomplete-arch

ABSTRACT

Objectives: To investigate the trueness of intraoral photogrammetry (IPG) technology for complete-arch implant digital impression and evaluate the effect of implant number.

Material and Methods: All data were fully anonymized in compliance with ethical standards, and a total of 30 complete-arch patient models with 4 ($n = 13$), 5 ($n = 9$), or 6 ($n = 8$) implants were selected from the archive. Digital impressions were taken with IPG and a desktop scanner. Test and reference standard tessellation language (STL) files were superimposed using a best-fit algorithm. For each implant position, mean linear (ΔX , ΔY , ΔZ axes) and angular deviations (ΔANGLE) and three-dimensional (3D) Euclidean distances (ΔEUC) were measured as primary outcomes with a dedicated software program (Hyper Cad S, Cam HyperMill, Open Mind Technologies) and reported as descriptive statistics. Secondary aim was to determine using linear mixed models whether implant number affected trueness. All statistical analyses were conducted using Stata 18 (Stata Corp, College Station) and significance was set at 0.05.

Results: A total of 30 definitive casts with 4 ($n = 13$), 5 ($n = 8$), and 6 ($n = 9$) multi-unit abutment (MUA) analogs were analyzed ($n = 146$ implant positions). The mean deviations along the X -axis were $-3.97 \pm 32.8 \mu\text{m}$, while along the Y -axis, they were $-1.97 \pm 25.03 \mu\text{m}$. For the Z -axis, a greater deviation of $-33 \pm 34.77 \mu\text{m}$ was observed. The 3D Euclidean distance deviation measured $57.22 \pm 27.41 \mu\text{m}$, and the angular deviation was $0.26^\circ \pm 0.19^\circ$. Statistically significant deviations were experienced for ΔZ , ΔEUC , and ΔANGLE ($p < 0.01$). Additionally, the number of implants had a statistically significant effect only on the Z -axis deviation ($p = 0.03$).

Conclusions: Within study limitations, IPG technology was feasible for complete-arch digital implant impression with mean linear, angular, and 3D deviations far below the acceptable range for a passive fit. Reported IPG trueness might avoid a rigid prototype try-in. The implant number had no influence on trueness except for Z -axis deviations. Integrating photogrammetry with intraoral optical scanning (IOS) improved practicality, optimizing the digital workflow. Further clinical trials are needed to confirm these findings.

This is an open access article under the terms of the [Creative Commons Attribution-NonCommercial-NoDerivs](https://creativecommons.org/licenses/by-nc-nd/4.0/) License, which permits use and distribution in any medium, provided the original work is properly cited, the use is non-commercial and no modifications or adaptations are made.

© 2025 The Author(s). *Clinical Implant Dentistry and Related Research* published by Wiley Periodicals LLC.

1 | Introduction

Accurate recording of implant positions is essential for achieving a precise fit of complete-arch fixed dental prostheses (FDP) [1–3]. Conventional intraoral optical scanning (IOS) has been widely used for digital impressions, but struggles with accuracy in complete-arch implant cases [1, 4–7]. While IOS performed reliably for single crowns and short-span restorations [8], its accuracy diminishes over larger spans due to stitching errors and scan misalignment [1, 7]. Consequently, its use for definitive complete-arch FDP remains controversial [9–15].

To overcome these limitations and enhance IOS accuracy in complete-arch cases, different techniques were developed [5, 10, 16]. However, the use of IOS impression remained controversial for definitive complete-arch FDPs. While some studies report improved accuracy with these techniques [5, 15, 17–19] others find no significant differences or even reduced accuracy [19–22]. Given the need for high accuracy in complete-arch implant capture [23, 24], innovative technologies such as extraoral photogrammetry (EPG) were introduced [18, 25, 26].

EPG uses stereo cameras to detect fiducial geometries on intraoral scan bodies (SBs), ensuring accurate three-dimensional (3D) spatial relationships [27]. Studies have reported EPG's superior accuracy over IOSs, but most research has been in vitro, limiting its clinical applicability [25, 28, 29]. Latest evidence in vivo comparing IOS with EPG confirmed the latter as superior in accuracy, even though further clinical trials are needed to achieve a consensus [26]. Moreover, EPG only records implant positions, requiring an additional IOS scan to capture soft tissue, upper and lower arch anatomy, and their bite relationship, making the complete-arch digital workflow complex [27, 29–31] and costly due to the need for two different technologies to capture all the intraoral data needed for the prosthetic process [26, 32].

A new intraoral device, integrating IOS with photogrammetry (IPG), was recently introduced. Unlike previous methods that required separate ISBs and manual alignment, this device automatically generates a single STL file that includes implant positions, jaw anatomy, and occlusion in one scan. By combining the accuracy of photogrammetry with IOS's ability to capture soft tissue, IPG may offer a more practical and efficient approach to complete-arch digital implant impressions.

To the best of our knowledge, this is the first study evaluating IPG trueness on actual patient models. The primary aim was to assess linear, 3D, and angular deviations (trueness), while the secondary aim was to determine whether implant number (4, 5, or 6) affected trueness. The first null hypothesis stated that there would be no significant difference between IPG impressions and the reference files. The second null hypothesis stated that the number of implants per model (4, 5, and 6) would not significantly affect IPG trueness.

2 | Materials and Methods

American Dental Association (ADA) type IV dental stone definitive casts with 4, 5, and 6 implants were randomly selected from an existing archive of anonymized records of patients treated



FIGURE 1 | Novel intraoral photogrammetry (IPG) device—Elite, Shining 3D.



FIGURE 2 | IPG workflow: Surrounding implant tissue scanning.

with complete-arch FDPs. No identifiable patient information was used, and all data were fully anonymized in compliance with ethical standards. The archive is a collection of actual dental casts, belonging to patients who had given prior consent for their anonymized data to be used for research purposes. Peer review of empirical data was conducted by an independent examiner and member of the scientific committee of the University of Rome Tor Vergata to confirm the quality of the shared data and to confirm that the data reproduce the analytic results reported in this article. Each model contained multi-unit abutment (MUA) replicas (Nobel Biocare) and was scanned using both the investigated IPG device (Elite, Shining 3D) (Figure 1) and a high-resolution desktop scanner to achieve a test scan and a reference scan for each model. The IPG device, as declared by the producers, integrates IPG technology within a handheld intraoral device equipped with two cameras: one for intraoral surface scanning and another for photogrammetry.

The IPG scanning process included three main steps:

1. Capturing soft tissue anatomy using a scanning strategy reported for edentulous patients' adherent to manufacturer's instructions for use. (Figure 2).
2. Detecting and positioning ISBs onto MUAs with a 10Ncm torque wrench. Proper seating was visually confirmed. The ISBs had a hexagonal vertical shape and a multi-faceted horizontal part with black-and-white fiducial markers for accurate recognition (Figure 3). To ensure simultaneous capture, ISBs of different lengths (long, medium, short)



FIGURE 3 | Picture of IPG SBs screwed during the impression.

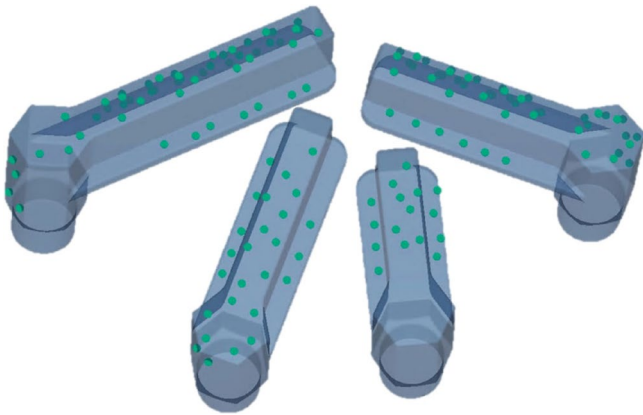


FIGURE 4 | IPG workflow: IPG scan bodies (SB) impression.

were arranged in a radial pattern without touching each other. The IPG software automatically identified and matched ISBs with their digital geometry (Figure 4).

3. Aligning the digital geometry of SB to the surrounding soft tissue, with two different scans, one for each side of the arch. This enabled automatic merging of the anatomical data from Step 1 with ISB positions from Step 2 (Figures 5 and 6).
4. Exporting implant positions after the impression was completed. Since IPG software does not export proprietary ISB geometries, implant coordinates were transferred into the test STL file using an open export function, selecting compatible ISB geometries from available dental market options (Figures 7 and 8).

For reference scans, definitive casts were digitized using a high-resolution extraoral desktop scanner (Autoscan DS-EX Pro(H), Shining 3D), with an accuracy of $8\mu\text{m}$ declared by the producer, as specified by the International Organization for Standardization, 2012 (ISO) standard 12836 [33]. This scanner was selected due to its high reported accuracy, stability in controlled environments, and its frequent use as a gold standard in dental research for evaluating the trueness of intraoral scanning methods. Moreover, a desktop scanner is the most



FIGURE 5 | IPG workflow: Merging of SB with surrounding tissues on the left side.

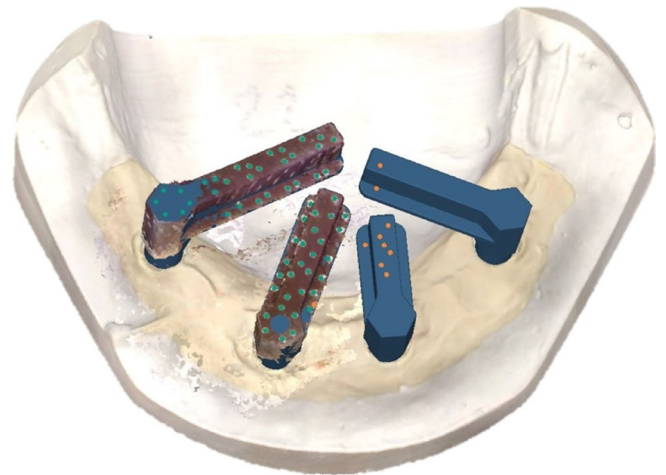


FIGURE 6 | IPG workflow: Merging of SB with surrounding tissues on the right side.

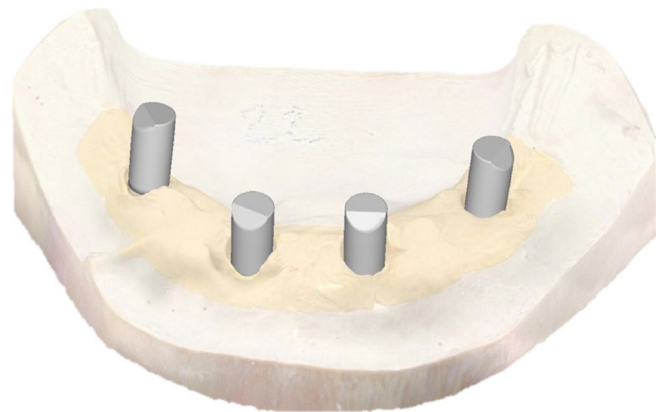


FIGURE 7 | IPG workflow: Standard tessellation language (STL) output of IPG SBs converted into commercially available intraoral SBs related to the surrounding tissue anatomy.

adopted technology to digitize the master cast by the dental laboratories and therefore we can assume that using such reference as a benchmark may enhance the translation of this study's

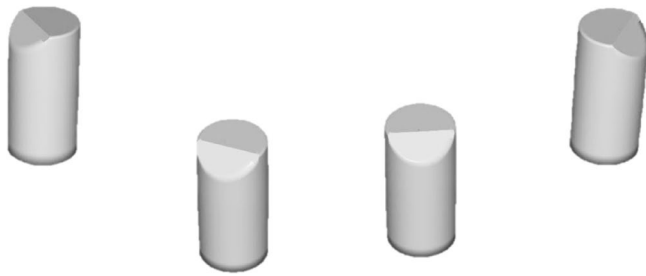


FIGURE 8 | IPG workflow: STL output of commercially available intraoral SBs alone.

outcomes to clinical reality [20, 22, 26]. The definitive casts were scanned by a properly trained operator who performed 30 IPG digital impressions. The scanning strategy adhered to the manufacturer's guidelines and was consistent throughout all digital scanning procedures. As the SBs were arranged radially with their tips converging medially, the scanning process initiated at the point of convergence of all SB tips, as illustrated in Figure 3. At this starting point, the field of view (FOV) of the IPG scanner encompassed multiple SBs simultaneously, and this allowed the software to interrelate since the beginning all the SB coordinates. Then the wand was moved radially along the multifaceted horizontal part of each SB up to the hexagonal vertical portion, before returning to the center. As the system detected the digital geometry, the dots on the surfaces turned green, as illustrated in Figure 4.

Reference STL files were generated by scanning the same ISBs visualized in the test scans. All digital scans were performed under controlled conditions, with ambient lighting standardized and room temperature maintained at 22°C. The scanning environment featured a non-reflective surface on which the casts were positioned and secured. No direct operative lighting was used; only the ceiling light fixture provided illumination, while external daylight was blocked to prevent light interference [34, 35].

The test STL files (showing implant positions) were aligned to their corresponding reference scans in a CAD (Computer Aided Design) software program (Exocad, Align Technology) initially using a point-based alignment by identifying corresponding points on the surfaces (i.e., head of the SB) to bring them closer. A best-fit algorithm was used then to refine the alignment of the geometries, with a tolerance of 0.01 mm. Mean linear deviations (ΔX , ΔY , and ΔZ) and angular deviations (ΔANGLE) were measured for each implant position using a dedicated

software program (Hyper Cad S, Cam HyperMill, Open Mind Technologies). Negative values on the X, Y, and Z axes indicated implants positioned left, downwards, and backward, respectively (lateral, longitudinal, and vertical), while positive values represented the opposite directions on each axis. The 3D deviation was calculated for each implant position using the Euclidean distance formula (ΔEUC).

A sample size calculation was performed assuming Euclidean distance (ΔEUC) as the primary endpoint, as it provides a comprehensive measure of 3D deviations by integrating linear differences across all axes. A clinically relevant effect size of 120 μm (SD: 150 μm) was selected based on prior research on complete-arch implant trueness [26] and accepted accuracy thresholds for passive fit [36]. With a significance level of 0.05 and a test power of 90%, a minimum of 66 implants ($n = 66$) was required.

Descriptive statistics were calculated for ΔX (μm), ΔY (μm), ΔZ (μm), ΔEUC (μm) and ΔANGLE ($^\circ$). To evaluate whether the deviations from the reference were statistically significantly different, a series of linear mixed models (random intercept) were fitted. Marginal plots were generated to illustrate mean deviations with 95% confidence intervals. Additional linear mixed models (random intercept) were used to examine the effect of implant number on the overall trueness. All statistical analyses were conducted using Stata 18 (Stata Corp, College Station).

3 | Results

Thirty definitive casts of complete-arch implant patients with six ($n = 9$), five ($n = 8$), and four ($n = 13$) MUA implant replicas were analyzed ($n = 146$ implant positions). Deviations for each ISB were evaluated along the X, Y, and Z axes, as well as in 3D Euclidean distance and angular deviations. The descriptive analysis results, both overall and stratified by implant number, were presented in Tables 1 and 2. These results indicate relatively small deviations along the X ($-3.97 \pm 32.8 \mu\text{m}$) and Y ($-1.97 \pm 25.03 \mu\text{m}$) axes, whereas the Z-axis exhibited larger deviations ($-33 \pm 34.77 \mu\text{m}$). The mean 3D linear deviation (ΔEUC) was $57.22 \pm 27.41 \mu\text{m}$, and the mean angular deviation was $0.26^\circ \pm 0.19^\circ$. Across all definitive casts, the Z-axis (vertical) consistently expressed the highest deviations compared to the Y (lateral) and X axes. The deviations between the IPG and the desktop scanner were analyzed using predictive margins with 95% confidence intervals (CIs), as shown in Table 3 and Figure 9. Statistically significant differences were observed in Z-axis deviations (ΔZ), ΔEUC , and ΔANGLE ($p < 0.01$). When trueness was stratified by implant number (4, 5,

TABLE 1 | Descriptive analysis of overall linear and angular deviations.

	Mean	Standard deviation	Range (min–max)	75 percentile
ΔX (μm)	−3.97	32.8	−85.62–71.11	19.34
ΔY (μm)	−1.97	25.03	−81.10–56.17	15.71
ΔZ (μm)	−33.3	34.77	−136.50–33.39	−0.87
ΔEUC (μm)	57.22	27.41	5.50–138.00	73.73
ΔAngle ($^\circ$)	0.26	0.19	0.01–1.00	0.33

TABLE 2 | Descriptive analysis stratified by implant number.

Mean (standard deviation)					
Model	ΔX (μm)	ΔY (μm)	ΔZ (μm)	ΔEUC (μm)	ΔAngle
4I	1.1 (32.6)	−0.9 (24.1)	31.3 (34.9)	55.1 (27.7)	0.27 (0.18)
5I	−5.6 (33.8)	−0.8 (27.0)	19.6 (28.9)	50.8 (22.0)	0.27 (0.20)
6I	−8.1 (32.1)	−3.4 (24.7)	45.4 (34.7)	63.9 (29.5)	0.25 (0.18)

TABLE 3 | Deviations from reference per variables: p values.

	ΔX	ΔY	ΔZ	ΔEUC	ΔAngle
p	0.13	0.39	<0.01	<0.01	<0.01

and 6 implants), only Z -axis deviations showed statistically significant differences ($p=0.03$), indicating a potential impact of implant number on vertical trueness (Figure 10 and Table 4).

4 | Discussion

The present in vitro study investigated real patient definitive casts for the trueness of a novel complete-arch implant digital impression technology that integrates photogrammetry and optical surface scanning within a handheld intraoral device. The IPG system captured all impressions without errors, using AI-driven software to detect and recognize coded ISBs, thereby

integrating implant coordinates with surface optical scanning. A key limitation of this study was its in vitro design, which does not fully replicate clinical conditions such as the presence of oral fluids, anatomic interference (tongue, cheeks, lips), lack of keratinized tissue, patient-specific anatomical variations, and movement [37]. However, unlike studies using a single artificial dental cast, this research was conducted on real patient definitive casts with varying implant numbers, positions, and angulations, potentially enhancing clinical relevance. Another limitation might be related to the use of a certified desktop scanner as the reference, though extraoral optical scanning is widely regarded as superior to IOS due to the controlled environment and advanced optical systems, and it is used as a standard laboratory procedure for digitizing dental casts and for CAD-CAM (Computer Aided Manufacturing) fabrication of complete-arch FDPs [22, 26].

The clinical implications of these findings suggested that IPG technology may enhance the predictability of complete-arch

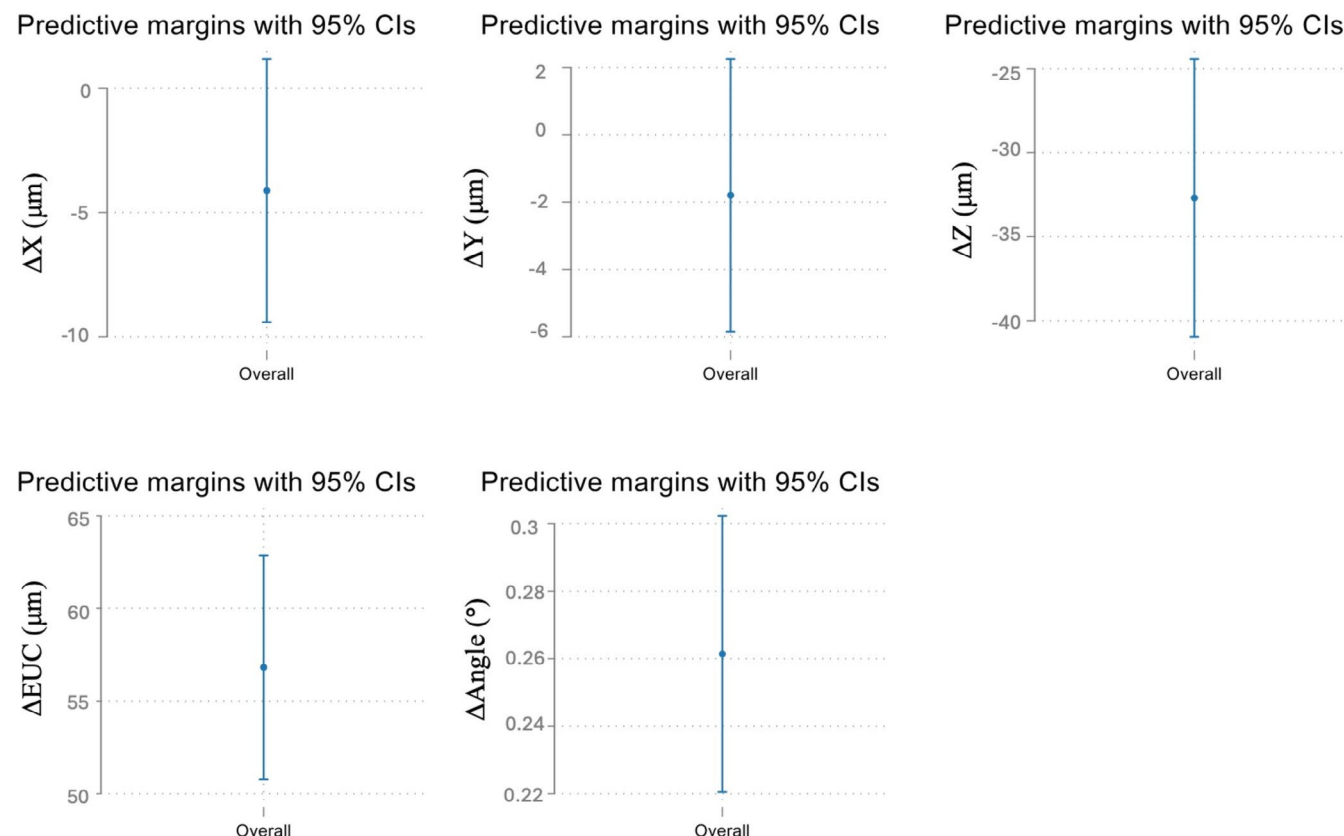


FIGURE 9 | Deviations from the gold standard per variable: Mean and 95% confidence intervals.

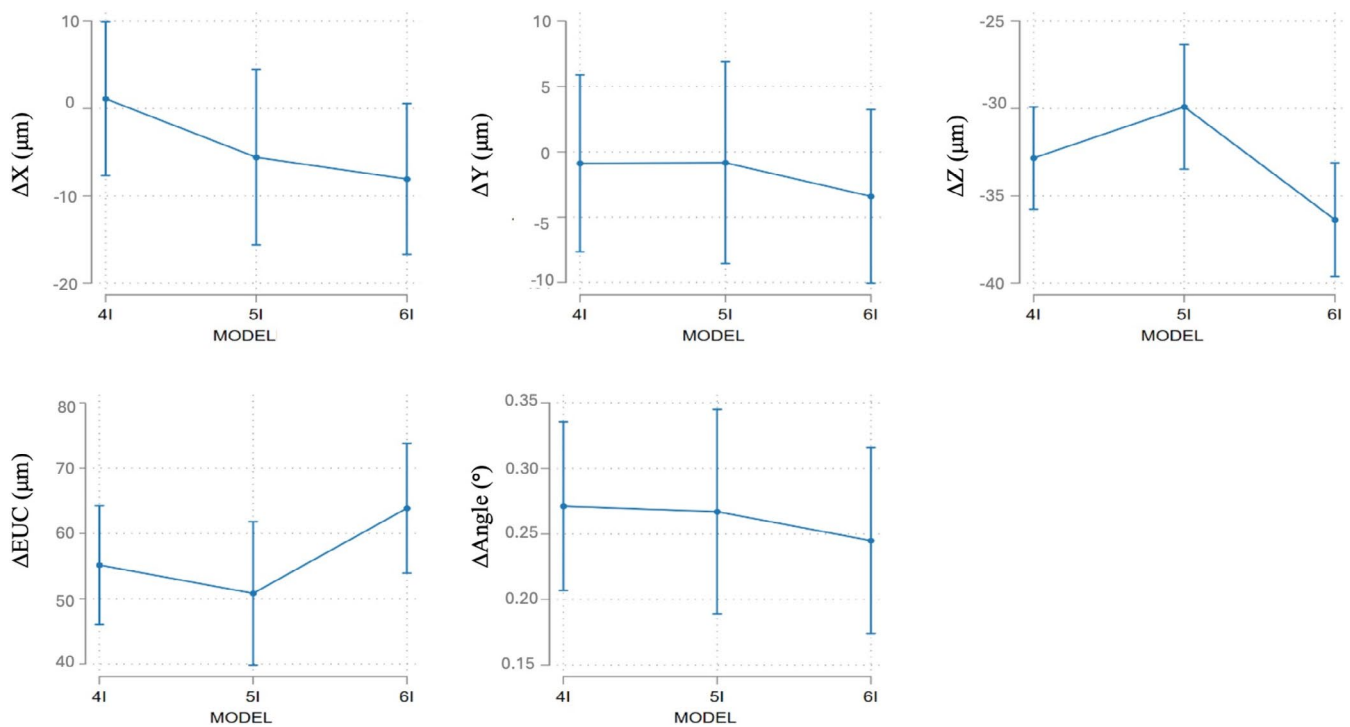


FIGURE 10 | Effect of the number of implants on overall accuracy.

TABLE 4 | Effect of the number of implants on overall accuracy: p values.

	ΔX	ΔY	ΔZ	ΔEUC	$\Delta Angle$
p	0.32	0.84	0.03	0.20	0.85

implant FDP by providing highly accurate digital impressions. Therefore, a rigid prototype try-in might be avoided before manufacturing a definitive prosthesis if the reported outcomes remain consistent in an *in vivo* context. The IPG trueness may facilitate the CAD-CAM production of a passive fit screw-retained FDP, reducing the need for manual adjustments and streamlining the overall prosthesis fabrication process. Additionally, the ability to improve the digital workflow may enhance treatment efficiency, leading to shorter treatment times and fewer clinical visits, ultimately benefiting both patients and clinicians. Furthermore, the IPG scanning protocol closely mirrored the traditional IOS wand movements along the dental arch, thus minimizing the need for a steep learning curve.

To the best of the authors' knowledge, this is the first study assessing the trueness of IPG-based complete-arch implant digital impressions on actual patient models using a statistically powered sample size calculation. Based on the results, the first null hypothesis was rejected, as IPG deviations in the Z-axis, ΔEUC , and $\Delta ANGLE$ were significantly different from the reference ($p < 0.01$). However, despite statistical significance, these deviations ($\Delta Z -33.3 \pm 34.77$, $\Delta EUC 57.22 \pm 27.41 \mu m$, and $\Delta ANGLE 0.26^{\circ} \pm 0.19^{\circ}$) remained well below the clinically acceptable thresholds for passive fit ($150 \mu m$ and 1°) [36]. Even in extreme cases, deviations did not exceed these limits (Table 1). The second null hypothesis was partially rejected, as implant number influenced only the Z-axis deviations ($p = 0.03$), with no

significant effect on ΔX , ΔY , ΔEUC , or $\Delta ANGLE$. Recently, IPG accuracy was investigated and compared with EPG [38] and IOS [39]. Revilla-Leon et al. (2025) measured the Euclidean linear distance among the SBs reporting a lower mean linear deviation of $27 \pm 5 \mu m$ and a similar mean angular discrepancy of $0.27^{\circ} \pm 0.02^{\circ}$ between IPG and the desktop scanner reference file, compared to our findings. This more favorable linear deviation may be attributed to differences in research methodology, as the previous study examined a single artificial model with only one implant configuration. In contrast, the present study assessed IPG trueness across 30 real complete-arch cases, incorporating variations in soft tissue anatomy, implant number, positions, and angulations. As a result, the higher Euclidean mean deviation reported in this study may be more reliably translated to clinical settings compared to *in vitro* studies conducted on a single artificial cast with a fixed implant configuration.

Brakoč et al. (2025) assessed the accuracy of IPG as distance standard deviation, integrated distance, and integrated absolute distance, with IPG reporting the highest accuracy in all measured parameters compared to conventional IOS technologies.

Available studies on EPG vary significantly in methodology and reported outcomes. The EPG scanners were investigated using as reference various technologies such as laboratory and industrial optical scanners, and coordinate measuring machines (CMM), leading to a broad range of recorded deviations.

Additionally, different study parameters were analyzed, such as 3D, linear, and angular deviations, root mean square (RMS) values, and inter-implant distances. Nevertheless, comparisons with EPG systems revealed that IPG exhibited lower deviations along the X and Y axes but slightly higher deviations (by approximately $10 \mu m$) along the Z-axis compared to *in vitro* EPG [25].

IPG's 3D and angular deviations were slightly higher than EPG in vitro ($\Delta\text{EUC} = 33.42 \pm 7.71 \mu\text{m}$, $\Delta\text{ANGLE} = 0.24^\circ \pm 0.04^\circ$) but lower than conventional in vivo EPG ($\Delta\text{EUC} = 87.6 \pm 74.2 \mu\text{m}$, $\Delta\text{ANGLE} = 0.38^\circ \pm 0.29^\circ$) [26]. These findings highlighted the importance of evaluating new technologies under both in vitro and in vivo conditions, given that patient variability may impact outcomes. However, the present study was conducted on real patient implant models, with different characteristics, and such variability may have penalized the IPG outcomes with respect to EPG in vitro studies conducted on a single model. Furthermore, IPG showed higher trueness compared to IOS, which exhibited larger mean and extreme deviations in vitro and in vivo [26, 40].

Different strategies have been proposed to improve IOS accuracy, such as artificial landmarks, splinting of ISBs, horizontally designed ISBs, and CAD-designed auxiliary splinting devices, yet extreme deviations persist, suggesting the need of use of try-ins before final prosthesis superstructure fabrication [17, 40–43]. All these strategies were developed to create a scanning route for the IOS digital impression that may facilitate the multiple 3D stitching procedure. For the same reason, IPG coded SBs were designed with a vertical hexagonal and a rectangular multifaceted horizontal part. SBs were positioned to figure out a radial geometry without touching each other to ensure the simultaneous capture of multiple SB surfaces during the scanning, facilitating the detection of coded fiducial geometries and their match with the soft tissue anatomy of the edentulous patient. The IPG system integrates photogrammetry directly into an IOS device, facilitating implant coordinate acquisition and surface scanning in a single workflow. Unlike conventional EPG digital impressions, which capture only implant coordinates without intraoral soft tissue data, IPG consolidates all relevant information into a single dataset, improving CAD/CAM workflows for immediate prosthesis fabrication. Traditionally, a second impression, either through direct or indirect digitalization, was required to merge implant positions with the surrounding soft tissues and create a complete digital master model.

By integrating both IOS and photogrammetry into a single device, IPG eliminates the need for multiple technologies, potentially reducing overall equipment costs and simplifying clinical workflows. This dual functionality may lead to fewer patient visits, decreased chairside time, and reduced material consumption, improving cost-efficiency while maintaining accuracy. Additionally, as the world's first device to employ both digital impression technologies, IPG provides versatility for both edentate and edentulous cases, further enhancing its practicality in clinical settings.

Additionally, IPG allows open-format export, making it compatible with various implant ISB geometries from major manufacturers. Although the use of real patient dental casts supports cautious generalization, further clinical trials are needed to validate IPG's in vivo performance.

5 | Conclusion

Within study limitations, IPG technology was feasible for complete-arch digital implant impression with mean linear, angular, and 3D deviations far below the acceptable range for a

passive fit. Implant number had no influence on trueness except for Z-axis deviations. Integrating photogrammetry with IOS improved practicality, optimizing the digital workflow. Further clinical trials are needed to confirm these findings.

Within the limitations of this in vitro study, intraoral photogrammetry was feasible for complete-arch implant digital impressions:

- IPG linear deviations along the X and Y axes were lower than conventional EPG deviations reported in previous in vitro and in vivo studies.
- Mean 3D linear (ΔEUC) and angular (ΔANGLE) deviations were far below the accepted thresholds for passive fit of complete-arch FDPs.
- The reported IPG trueness might avoid a rigid prototype try-in.
- Among all investigated variables, implant number had no influence on trueness except for Z-axis deviations.
- IPG technology, combining IOS and photogrammetry, optimizes the digital workflow for complete-arch implant impressions, potentially enhancing treatment efficiency by reducing treatment time and clinical visits, benefiting both patients and clinicians.
- The IPG scanning protocol closely mirrored the traditional IOS wand movements along the dental arch, thus minimizing the need for a steep learning curve.
- While real patient models allow for some generalization, further clinical trials are needed to better assess the clinical performance and reliability of this novel complete-arch digital impression technology.

Author Contributions

A.P. and A.L. conceived the ideas, collected the data, analyzed the data, and wrote the manuscript. I.T. conceived the ideas, found the resources and materials. L.A. and J.C. validated the analysis, supervised the study, and reviewed the manuscript. V.F. and I.S. supervised, reviewed, and edited the manuscript.

Acknowledgments

The authors thank Prof. Nikolaos Pandis for the statistical support. The authors also thank the Shining 3D company for providing the investigated device.

Conflicts of Interest

The authors declare no conflicts of interest.

Data Availability Statement

The data that support the findings of this study are available from the corresponding author upon reasonable request.

References

1. V. Rutkūnas, A. Gečiauskaitė, D. Jegelevičius, and M. Vaitiekūnas, "Accuracy of Digital Implant Impressions With Intraoral Scanners:

- A Systematic Review,” *European Journal of Oral Implantology* 10, no. Suppl 1 (2017): 101–120.
2. A. Pozzi, L. Arcuri, F. Lio, et al., “Accuracy of Complete-Arch Digital Implant Impression With or Without Scanbody Splinting: An In Vitro Study,” *Journal of Dentistry* 125 (2022): 104072, <https://doi.org/10.1016/j.jdent.2022.104072>.
 3. G. Pradíes, A. Ferreiroa, M. Özcan, B. Giménez, and F. Martínez-Rus, “Using Stereophotogrammetric Technology for Obtaining Intraoral Digital Impressions of Implants,” *Journal of the American Dental Association* (1939) 145, no. 4 (2014): 338–344, <https://doi.org/10.14219/jada.2013.45>.
 4. M. Sanda, K. Miyoshi, and K. Baba, “Trueness and Precision of Digital Implant Impressions by Intraoral Scanners: A Literature Review,” *International Journal of Implant Dentistry* 7, no. 1 (2021): 97, <https://doi.org/10.1186/s40729-021-00352-9>.
 5. A. Pozzi, M. Tallarico, F. Mangani, and A. Barlattani, “Different Implant Impression Techniques for Edentulous Patients Treated With CAD/CAM Complete-Arch Prostheses: A Randomized Controlled Trial Reporting Data at 3-Year Post-Loading,” *European Journal of Oral Implantology* 6, no. 4 (2013): 325–340.
 6. S. Amin, H. P. Weber, M. Finkelman, K. el Rafie, Y. Kudara, and P. Papaspyridakos, “Digital vs. Conventional Full-Arch Implant Impressions: A Comparative Study,” *Clinical Oral Implants Research* 28, no. 11 (2017): 1360–1367, <https://doi.org/10.1111/clr.12994>.
 7. T. Flügge, W. J. van der Meer, B. G. Gonzalez, K. Vach, D. Wismeijer, and P. Wang, “The Accuracy of Different Dental Impression Techniques for Implant-Supported Dental Prostheses: A Systematic Review and Meta-Analysis,” *Clinical Oral Implants Research* 29, no. S16 (2018): 374–392, <https://doi.org/10.1111/clr.13273>.
 8. M. Imburgia, S. Logozzo, U. Hauschild, G. Veronesi, C. Mangano, and F. G. Mangano, “Accuracy of Four Intraoral Scanners in Oral Implantology: A Comparative In Vitro Study,” *BMC Oral Health* 17, no. 1 (2017): 92, <https://doi.org/10.1186/s12903-017-0383-4>.
 9. H. Tohme, G. Lawand, R. Eid, K. E. Ahmed, Z. Salameh, and J. Makzoume, “Accuracy of Implant Level Intraoral Scanning and Photogrammetry Impression Techniques in a Complete Arch With Angled and Parallel Implants: An In Vitro Study,” *Applied Sciences* 11, no. 21 (2021): 9859, <https://doi.org/10.3390/app11219859>.
 10. A. Blanco-Plard, A. Hernandez, F. Pino, et al., “3D Accuracy of a Conventional Method Versus Three Digital Scanning Strategies for Completely Edentulous Maxillary Implant Impressions,” *International Journal of Oral and Maxillofacial Implants* 6 (2023): 1211–1219, <https://doi.org/10.11607/jomi.10266>.
 11. A. G. Jasim, M. G. Abo Elezz, G. Y. Altonbary, and M. A. Elsyad, “Accuracy of Digital and Conventional Implant-Level Impression Techniques for Maxillary Full-Arch Screw-Retained Prosthesis: A Crossover Randomized Trial,” *Clinical Implant Dentistry and Related Research* 26, no. 4 (2024): 714–723, <https://doi.org/10.1111/cid.13336>.
 12. M. Gómez-Polo, A. Sallorenzo, R. Cascos, J. Ballesteros, A. B. Barmak, and M. Revilla-León, “Conventional and Digital Complete Arch Implant Impression Techniques: An In Vitro Study Comparing Accuracy,” *Journal of Prosthetic Dentistry* 132, no. 4 (2024): 809–818, <https://doi.org/10.1016/j.prosdent.2022.08.028>.
 13. B. Albayrak, C. Sukotjo, A. G. Wee, İ. H. Korkmaz, and F. Bayındır, “Three-Dimensional Accuracy of Conventional Versus Digital Complete Arch Implant Impressions,” *Journal of Prosthodontics* 30, no. 2 (2021): 163–170, <https://doi.org/10.1111/jopr.13264>.
 14. P. Kosago, C. Ungurawasaporn, and B. Kukiattrakoon, “Comparison of the Accuracy Between Conventional and Various Digital Implant Impressions for an Implant-Supported Mandibular Complete Arch-Fixed Prosthesis: An In Vitro Study,” *Journal of Prosthodontics* 32, no. 7 (2023): 616–624, <https://doi.org/10.1111/jopr.13604>.
 15. N. J. Marshaha, A. A. Azhari, M. K. Assery, and W. M. Ahmed, “Evaluation of the Trueness and Precision of Conventional Impressions Versus Digital Scans for the All-On-Four Treatment in the Maxillary Arch: An In Vitro Study,” *Journal of Prosthodontics* 33, no. 2 (2024): 171–179, <https://doi.org/10.1111/jopr.13666>.
 16. Y. Ashraf, A. Abo El Fadl, A. Hamdy, and K. Ebeid, “Effect of Different Intraoral Scanners and Scanbody Splinting on Accuracy of Scanning Implant-Supported Full Arch Fixed Prosthesis,” *Journal of Esthetic and Restorative Dentistry* 35, no. 8 (2023): 1257–1263, <https://doi.org/10.1111/jerd.13070>.
 17. L. Retana, A. H. Nejat, and A. Pozzi, “Effect of Splinting Scan Bodies on Trueness of Complete-Arch Implant Impression Using Different Intraoral Scanners: An In Vitro Study,” *International Journal of Computerized Dentistry* 26, no. 1 (2023): 19–28, <https://doi.org/10.3290/j.jcd.b2599297>.
 18. V. Rutkunas, “Accuracy of Photogrammetry Devices, Intraoral Scanners, and Conventional Techniques for the Full-Arch Implant Impressions: A Systematic Review,” *European Journal of Prosthodontics and Restorative Dentistry* 31, no. 1 (2023): 1–10, https://doi.org/10.1922/EJPRD_2481Rutkunas12.
 19. K. Chochlidakis, P. Papaspyridakos, A. Tsigarida, et al., “Digital Versus Conventional Full-Arch Implant Impressions: A Prospective Study on 16 Edentulous Maxillae,” *Journal of Prosthodontics* 29, no. 4 (2020): 281–286, <https://doi.org/10.1111/jopr.13162>.
 20. L. Azevedo, T. Marques, D. Karasan, et al., “Effect of Splinting Scan Bodies on the Trueness of Complete Arch Digital Implant Scans With 5 Different Intraoral Scanners,” *Journal of Prosthetic Dentistry* 1 (2024): 204–210, <https://doi.org/10.1016/j.prosdent.2023.06.015>.
 21. K. Ali, A. A. Alzaid, M. S. Suprono, A. Garbacea, R. Savignano, and M. T. Kattadiyil, “Evaluating the Effects of Splinting Implant Scan Bodies Intraorally on the Trueness of Complete Arch Digital Scans: A Clinical Study,” *Journal of Prosthetic Dentistry* 132, no. 4 (2024): 781, <https://doi.org/10.1016/j.prosdent.2024.03.004>.
 22. R. M. Mizumoto, B. Yilmaz, E. A. McGlumphy, J. Seidt, and W. M. Johnston, “Accuracy of Different Digital Scanning Techniques and Scan Bodies for Complete-Arch Implant-Supported Prostheses,” *Journal of Prosthetic Dentistry* 123, no. 1 (2020): 96–104, <https://doi.org/10.1016/j.prosdent.2019.01.003>.
 23. M. Revilla-León, D. E. Kois, and J. C. Kois, “A Guide for Maximizing the Accuracy of Intraoral Digital Scans. Part 1: Operator Factors,” *Journal of Esthetic and Restorative Dentistry* 34, no. 1 (2022): 230–240, <https://doi.org/10.1111/jerd.12985>.
 24. M. Revilla-León, D. E. Kois, and J. C. Kois, “A Guide for Maximizing the Accuracy of Intraoral Digital Scans: Part 2—Patient Factors,” *Journal of Esthetic and Restorative Dentistry* 35, no. 1 (2023): 241–249, <https://doi.org/10.1111/jerd.12993>.
 25. A. Pozzi, E. Agliardi, F. Lio, K. Nagy, A. Nardi, and L. Arcuri, “Accuracy of Intraoral Optical Scan Versus Stereophotogrammetry for Complete-Arch Digital Implant Impression: An In Vitro Study,” *Journal of Prosthodontic Research* 68, no. 1 (2024): 172–180, https://doi.org/10.2186/jpr.JPR_D_22_00251.
 26. A. Pozzi, P. Carosi, G. O. Gallucci, K. Nagy, A. Nardi, and L. Arcuri, “Accuracy of Complete-Arch Digital Implant Impression With Intraoral Optical Scanning and Stereophotogrammetry: An In Vivo Prospective Comparative Study,” *Clinical Oral Implants Research* 34, no. 10 (2023): 1106–1117, <https://doi.org/10.1111/clr.14141>.
 27. R. Agustín-Panadero, D. Peñarrocha-Oltra, S. Gomar-Vercher, and M. Peñarrocha-Diago, “Stereophotogrammetry for Recording the Position of Multiple Implants: Technical Description,” *International Journal of Prosthodontics* 28, no. 6 (2015): 631–636, <https://doi.org/10.11607/ijp.4146>.
 28. B. Ma, X. Yue, Y. Sun, L. Peng, and W. Geng, “Accuracy of Photogrammetry, Intraoral Scanning, and Conventional Impression Techniques for Complete-Arch Implant Rehabilitation: An In Vitro Comparative Study,” *BMC Oral Health* 21 (2021): 636, <https://doi.org/10.1186/s12903-021-02005-0>.

29. H. Tohme, G. Lawand, M. Chmielewska, and J. Makhzoume, "Comparison Between Stereophotogrammetric, Digital, and Conventional Impression Techniques in Implant-Supported Fixed Complete Arch Prostheses: An In Vitro Study," *Journal of Prosthetic Dentistry* 129, no. 2 (2023): 354–362, <https://doi.org/10.1016/j.prosdent.2021.05.006>.
30. T. Jemt, T. Bäck, and A. Petersson, "Photogrammetry—An Alternative to Conventional Impressions in Implant Dentistry? A Clinical Pilot Study," *International Journal of Prosthodontics* 12, no. 4 (1999): 363–368.
31. P. Molinero-Mourelle, W. Lam, R. Cascos-Sánchez, L. Azevedo, and M. Gómez-Polo, "Photogrammetric and Intraoral Digital Impression Technique for the Rehabilitation of Multiple Unfavorably Positioned Dental Implants: A Clinical Report," *Journal of Oral Implantology* 45, no. 5 (2019): 398–402, <https://doi.org/10.1563/aaid-joi-D-19-00140>.
32. M. Revilla-León, W. Att, M. Özcan, and J. Rubenstein, "Comparison of Conventional, Photogrammetry, and Intraoral Scanning Accuracy of Complete-Arch Implant Impression Procedures Evaluated With a Coordinate Measuring Machine," *Journal of Prosthetic Dentistry* 125, no. 3 (2021): 470–478, <https://doi.org/10.1016/j.prosdent.2020.03.005>.
33. International Organization for Standardization, "ISO 12836:2015. Dentistry—Digitizing Devices for CAD/CAM Systems for Indirect Dental Restorations—Test Methods for Assessing Accuracy," accessed 02-01-20, <https://www.iso.org/standard/68414.html>.
34. M. Revilla-León, A. Gohil, A. B. Barmak, et al., "Influence of Ambient Temperature Changes on Intraoral Scanning Accuracy," *Journal of Prosthetic Dentistry* 130, no. 5 (2023): 755–760, <https://doi.org/10.1016/j.prosdent.2022.01.012>.
35. M. Revilla-León, S. G. Subramanian, M. Özcan, and V. R. Krishnamurthy, "Clinical Study of the Influence of Ambient Light Scanning Conditions on the Accuracy (Trueness and Precision) of an Intraoral Scanner," *Journal of Prosthodontics* 29, no. 2 (2019): 107–113, <https://doi.org/10.1111/jopr.13135>.
36. T. Jemt and A. Lie, "Accuracy of Implant-Supported Prostheses in the Edentulous Jaw: Analysis of Precision of Fit Between Cast Gold-Alloy Frameworks and Master Casts by Means of a Three-Dimensional Photogrammetric Technique," *Clinical Oral Implants Research* 6, no. 3 (1995): 172–180, <https://doi.org/10.1034/j.1600-0501.1995.060306.x>.
37. V. Rutkūnas, A. Gedrimienė, M. Akulauskas, et al., "In Vitro and In Vivo Accuracy of Full-Arch Digital Implant Impressions," *Clinical Oral Implants Research* 32, no. 12 (2021): 1444–1454, <https://doi.org/10.1111/clr.13844>.
38. M. Revilla-León, M. Gómez-Polo, M. Drone, A. B. Barmak, J. C. Koïs, and J. Alonso Pérez-Barquero, "Accuracy of Complete Arch Implant Scans Recorded by Using Intraoral and Extraoral Photogrammetry Systems," *Journal of Prosthetic Dentistry* 25 (2025): 00084, <https://doi.org/10.1016/j.prosdent.2025.01.041>.
39. J. Brakoč, A. Todorović, F. G. Mangano, M. Glišić, and M. Šćepanović, "Accuracy of Intraoral Photogrammetry Versus Direct Digital Implant Impressions in the Fully Edentulous Lower Jaw: An In Vitro Study," *Journal of Dentistry* 156 (2025): 105654, <https://doi.org/10.1016/j.jdent.2025.105654>.
40. L. Arcuri, A. Pozzi, F. Lio, E. Rompen, W. Zechner, and A. Nardi, "Influence of Implant Scanbody Material, Position, and Operator on the Accuracy of Digital Impression for Complete-Arch: A Randomized In Vitro Trial," *Journal of Prosthodontic Research* 64, no. 2 (2020): 128–136, <https://doi.org/10.1016/j.jpor.2019.06.001>.
41. P. Kanjanasavitree, P. Thammajaruk, and M. Guazzato, "Comparison of Different Artificial Landmarks and Scanning Patterns on the Complete-Arch Implant Intraoral Digital Scans," *Journal of Dentistry* 125 (2022): 104266, <https://doi.org/10.1016/j.jdent.2022.104266>.
42. R. Huang, Y. Liu, B. Huang, C. Zhang, Z. Chen, and Z. Li, "Improved Scanning Accuracy With Newly Designed Scan Bodies: An In Vitro Study Comparing Digital Versus Conventional Impression Techniques for Complete-Arch Implant Rehabilitation," *Clinical Oral Implants Research* 31, no. 7 (2020): 625–633, <https://doi.org/10.1111/clr.13598>.
43. J. Li, Z. Chen, P. Nava, S. Yang, J. Calatrava, and H. L. Wang, "Calibrated Intraoral Scan Protocol (CISP) for Full-Arch Implant Impressions: An In Vitro Comparison to Conventional Impression, Intraoral Scan, and Intraoral Scan With Scan-Aid," *Clinical Implant Dentistry and Related Research* 26, no. 5 (2024): 879–888, <https://doi.org/10.1111/cid.13338>.